

REACTION-RATE APPROACH TO NONRADIATIVE TRANSITIONS IN POLAR SOLIDS

M. Georgiev*

Instituto de Física, U.N.A.M., Apartado Postal 20-364,
Delegación Alvaro Obregón, 01000 México, D.F.

(recibido noviembre 8, 1984; aceptado noviembre 14, 1984)

ABSTRACT

A review is given of the basic concepts of the reaction-rate approach to nonradiative transitions in polar solids. The purpose of this paper is to call for the attention of the physicist through presenting a method that has first been introduced and applied to chemical problems. The reaction-rate theory is firmly based, simply formulated, and leads to immediate conclusions helping to easily reveal physics. It applies to a variety of nonradiative processes, involving the transfer of electrons or ions, between and including the extrema of adiabatic and nonadiabatic transitions. The paper is composed of three parts: Following a concise description of the method in Sections 2 and 3, applications to some specific experimental situations in ionic crystals are shown to demonstrate how it works. Among these are the vibrational properties of F centers in alkali halides, the relaxation of dipolar defects, and the hopping of self-trapped excitons. Practical ways to apply the method to deal with experimental rate data are advised.

* On leave of absence from the Institute of Solid State Physics, Bulgarian Academy of Sciences, Sofia, Bulgaria.

RESUMEN

Se presenta una revisión sobre los conceptos teóricos básicos de la razón-de-reacción aplicada a las transiciones no-radiativas en sólidos polares. El propósito del siguiente trabajo es llamar la atención de los físicos, al presentar un método que fue primero introducido y aplicado a problemas de la química. Esta teoría de la razón-de-reacción está fundamentada sobre bases sólidas, formulada de manera simple y conduce a conclusiones que revelan las bases físicas de los problemas. Esta teoría se puede aplicar a una gran variedad de procesos no-radiativos, incluyendo la transferencia de electrones o iones entre los valores extremos de transiciones adiabáticas o no-adiabáticas. El artículo se compone de tres partes: En las secciones 2 y 3 se presenta una descripción concisa del método, posteriormente se presentan aplicaciones del método a algunos resultados experimentales, específicamente a cristales iónicos. Entre ellas se encuentran las propiedades vibracionales del centro F en halogenuros alcalinos, la relajación de defectos dipolares y el salto de excitones auto-atrapados. Se explica la manera práctica de aplicar el método a resultados experimentales.

1. INTRODUCTION

The role of nonradiative transitions (NRT) in energy and matter transfer in solids has been appreciated for a long time. Phenomenologically a NRT is the process by which a system, initially under an external perturbation, relaxes to thermal equilibrium with the excess energy degrading in the form of heat. Among the large variety of NRT in solid state physics one can extract a few more typical examples:

- luminescence quenching (intra-or inter-center)
- free-carrier capture
- thermal ionization of excited electronic states
- spin-lattice relaxation
- production of lattice defects
- energy transfer
- diffusion
- dipolar reorientation, etc.

Even a first-sight inspection reveals the common features leading to two main groups of NRT in the above list involving: (i) an electron transfer from one state to another, such as free-carrier capture or intracenter luminescence quenching; and (ii) the net displacement of an electron or an

ionic defect from one site to another, such as diffusion and dipolar reorientation. In either case the NRT-undergoing entity interacts with the surrounding medium, which rearranges so as to make the transition possible. Later, a quantitative criterion will be introduced to distinguish between weakly (i) and strongly (ii) relaxed defect types. The increasing interest in studying NRT in solids is due to both their basic physical significance and practical importance.

It is by no means the purpose of this paper to present any comprehensive survey of NRT in solids; such reviews are already available in the literature.⁽¹⁻³⁾ We shall focus instead on a few cases that are both typical and instructive. A quantitative method will be presented for their description, and, hopefully, proper physical interpretation based on the reaction-rate approach.⁽⁴⁾ Although somewhat less familiar to the solid-state physicist, this method has widely been used in chemistry forming the basis of present-day understanding of chemical reactions. In addition to being both statistically justified and simply formulated, applying the reaction-rate method to deal with particular experimental situations would not require using sophisticated mathematical techniques. Having recently attended two major international conferences in the United States, on Luminescence and Defects in Insulating Crystals, the author is now well aware of the pressing need for a simpler theoretical approach that would enable the experimentalist to clearly interpret his data. Without pretending to be the magic torch, this paper is mainly aimed at demonstrating the virtues of a way alternative to the traditional multiphonon techniques.

The paper is further composed of three main parts. Following a general formulation of the eigenvalue problem, where an approximate solution of the Schrodinger equation for the electron-lattice system will be found within the adiabatic approximation, in Section 2, Section 3 will define the transition rate by means of the reaction-rate method, and will present relevant formulae for calculating the transition probabilities for a strongly-quantized system. Several examples will then be shown in Section 4 in which the theory has so far been found to compare favorably with experiments. Finally, the limitations of the theory at its present stage will be touched briefly and some practical prescriptions advised in the concluding part.

2. GENERAL FORMULATION OF THE EIGENVALUE PROBLEM

2.1. Hamiltonian

The excess energy in a nonradiative transition is given away to the (crystalline) medium through the interactions of electrons and lattice vibrations. This can be described properly only by means of quantum mechanics. We assume the medium to be polarizable and to be composed of a system of lattice oscillators performing vibrations around certain equilibrium positions. Due to the polarizability, the presence of any extra electron localized at some site in the crystal would displace the equilibrium positions of the oscillators, the magnitude of the displacement depending essentially on the spatial extension of the electron cloud, that is, on the electronic state. This displacement is the simplest manifestation of the existence of an electron-lattice interaction, arising from the polarizability, the interaction leading to a number of observable effects.

The Hamiltonian of a polarizable medium composed of electrons and oscillators will then read

$$H = H_e + H_L + H_{eL} \quad (2.1)$$

H_e is the static electronic Hamiltonian at fixed lattice, when all the oscillators are frozen-in at their equilibrium positions q_1^0 :

$$H_e = \sum_e \left(\frac{\vec{p}_e^2}{2 m_e} + V_e(\vec{r}_e; \tilde{q}^0) \right) \quad (2.2)$$

the sum being over the coordinates \vec{r}_e and momenta \vec{p}_e of all the electrons, m_e are the electron effective masses, $V_e(\vec{r}_e; \tilde{q}^0)$ is the static potential which the electrons "see" when the nuclei are at rest. When they are not, the electronic potential varies following parametrically the motion of the nuclei (adiabatic proposition). This modulated potential $V_e(\vec{r}_e; \tilde{q})$ can be expanded into a power series in q_1 , the nuclear coordinates (\tilde{q} is the manifold of all q_1), to give

$$V_e(\vec{r}_e; \tilde{q}) = V_e(\vec{r}_e; \tilde{q}^0) + \sum_1 (b_1(\vec{r}_e; q_1^0)(q_1 - q_1^0) + \dots, \quad (2.3)$$

The mixed electron-lattice terms in (2.3) effect the coupling of the electrons to the lattice oscillators. Consequently,

$$H_{eL} = \sum_{e, l, l'} (b_1(\vec{r}_e; q_1^0)(q_1 - q_1^0) + c_{11'}(\vec{r}_e; q_1^0, q_1^0, l')(q_1 - q_1^0)(q_1 - q_1^0, l') + \dots). \quad (2.4)$$

In the absence of an electron-lattice interaction the lattice Hamiltonian is

$$H_L = \sum_{l \neq l'} ((\vec{P}_1^2/2M_1) + \frac{1}{2}M_1\omega_1^2(q_1 - q_1^0)^2 + \frac{1}{2}M_1\omega_{11'}^2(q_1 - q_1^0)(q_1 - q_1^0, l') + \dots), \quad (2.5)$$

where M_1 , \vec{P}_1 , and ω_1 stand for the masses, momenta, and angular frequencies of the oscillators. The third term in (2.5) effects coupling between the oscillators which secures vibrational relaxation, and thereby thermal equilibrium, through the transfer of excitation energy to the heat reservoir of the lattice. This term introduces additional frequency dispersion of the oscillators. The intralattice coupling constants $\omega_{11'}$, are sometimes assumed small and the corresponding terms in Eq. (2.5) discarded from actual consideration when dealing with certain NRT types. However, being essential physically, these terms have always to be implied, if not taken into account explicitly. The Eq. (2.5) can be diagonalized in q_1^l :

$$H_L = \sum_1 ((P_1^2/2M_1) + \frac{1}{2}M_1\omega_1'^2(q_1^l - q_1^0)^2 + \dots) \quad (2.6)$$

to include the intralattice frequency dispersion. The equilibrium positions of the oscillators will further on be assumed to be at $q_1^0 = 0$, the origin of the lattice-configurational space. However, displacements from the origin of q_1^0 are induced by the electron-lattice coupling operators $b_1(\vec{r}_e, q_1^0)$ and $c_{11'}(\vec{r}_e, q_1^0, q_1^0, l')$. Of these, b_1 induce changes in the equilibrium positions, while $c_{11'}$ effect "electron-dressing" of the "bare" oscillators through changing the force constants.

To unravel the time-development of the system described by Eq. (2.1) solving Schrödinger's equation,

$$H \psi(\vec{r}_e, \tilde{q}) = E \psi(\vec{r}_e, \tilde{q}) \quad (2.7)$$

is required. However, the problem is largely complicated by the inclusion of electron-lattice coupling terms (2.4). This invokes the use of certain approximations.

2.2. Adiabatic approximation

According to the adiabatic theorem, an approximate solution to Eq. (2.7) may be sought in the form of the product

$$\psi(\vec{r}_e, \tilde{q}) = \psi_t(\vec{r}_e; \tilde{q}) \chi_{nt}(\tilde{q}) \quad , \quad (2.8)$$

of an electronic part ψ_t , which only depends parametrically on the nuclear coordinates \tilde{q} , times a vibrational part χ_{nt} , which depends on the electronic quantum numbers t as well. The parametric assumption is justified in cases where the electronic motion can be considered fast compared with the nuclear counterpart, to allow neglecting the dependence of ψ_t on the nuclear kinetic energy T_L . Such are the cases of localized electrons in solids whose orbital motion involves rotational frequencies much higher than the vibrational frequencies of the ions of the surrounding lattice, due to the large difference in the respective masses. Insofar as

$$T_L \psi_t(\vec{r}_e; \tilde{q}) \equiv \left[\sum_1 (\vec{p}_1^2 / 2M_1) \right] \psi_t(\vec{r}_e; \tilde{q}) = 0 \quad (2.9)$$

we define an "adiabatic Hamiltonian" by means of

$$H_{AD} = H - T_L \quad (2.10)$$

Inserting (2.8) into (2.7) we get

$$\begin{aligned} H(\psi\chi) &= H_{AD}(\psi\chi) + T_L(\psi\chi) \\ &= H_{AD}(\psi)\chi + (T_L\chi)\psi + T_L(\psi\chi) - (T_L\chi)\psi \quad . \end{aligned}$$

Putting now the parametric assumption (2.9) into force Eq. (2.7) splits

into two eigenvalue equations:

$$H_{AD}\psi_t(\tilde{\mathbf{r}}_e; \tilde{\mathbf{q}}) = E_t(\tilde{\mathbf{q}})\psi_t(\tilde{\mathbf{r}}_e; \tilde{\mathbf{q}}) \quad (2.11)$$

and

$$(T_L + E_t(\tilde{\mathbf{q}}))\chi_{nt}(\tilde{\mathbf{q}}) = E_{nt}\chi_{nt}(\tilde{\mathbf{q}}) \quad , \quad (2.12)$$

where E_{nt} are the eigenvalues of Eq. (2.7) in the adiabatic approximation. The complexity of the problem is, however, only partially reduced, since the electron-coupling terms remain in the operator part of Eq. (2.11). The residual expression

$$H' = T_L(\psi\chi) = (T_L\chi)\psi \quad , \quad (2.13)$$

vanishing under the parametric condition, is used as the NRT-driving operator in most multiphonon theories.

2.3. Diabatic hypersurfaces

Given a static electronic state $\psi_t(\tilde{\mathbf{r}}_e; \tilde{\mathbf{0}}) = |t; \tilde{\mathbf{0}}\rangle$, defined by

$$H_e|t; \tilde{\mathbf{0}}\rangle = E_t^0|t; \tilde{\mathbf{0}}\rangle \quad , \quad (2.14)$$

we find next the average value of H_{AD} to approximate for the eigenvalues of Eq. (2.11):

$$V_{tt}(\tilde{\mathbf{q}}) = \langle t; \tilde{\mathbf{0}} | H_{AD} | t; \tilde{\mathbf{0}} \rangle = \sum_1 \left[\frac{1}{2} M_1 \omega_1'^2 q_1'^2 + E_t^0 + b_{tt1} q_1' + c_{tt11} q_1'^2 + \dots \right] + \sum_1 \left[\frac{1}{2} M_1 \omega_{t1}''^2 (q_1'' - q_{t1}''^0)^2 + \dots \right] + Q_t \quad , \quad (2.15)$$

the second-order electron-lattice coupling tensor c_{11} , being assumed diagonalized prior to averaging. Here

$$b_{tt1} = \langle t; \tilde{\mathbf{0}} | \sum_{e,1} b_1(\tilde{\mathbf{r}}_e; \tilde{\mathbf{0}}) | t; \tilde{\mathbf{0}} \rangle \quad (2.16)$$

and

$$c_{tt11} = \langle t; \tilde{0} | \sum_{e,1} c_{11}(\vec{r}_e; \tilde{0}) | t; \tilde{0} \rangle \quad (2.17)$$

are the average values of the first- and second- order electron-lattice coupling operators, respectively,

$$q_{t1}''^0 = -b_{tt1} / M_1 \omega_{t1}''^2 \quad (2.18)$$

are the new equilibrium positions of the lattice oscillators, displaced because of the electron-lattice polarization interaction,

$$\omega_{t1}''^2 = \omega_1'^2 + 2c_{t11} / M_1 \quad (2.19)$$

are the new "electron-dressed" vibrational frequencies,

$$Q_t = E_t^0 - \sum_1 \frac{1}{2} M_1 \omega_{t1}''^2 (q_{t1}''^0)^2 \quad (2.20)$$

is the "electron-binding energy" in the adiabatic approximation. Remember that the frequency spectrum in (2.15) includes the induced intralattice coupling dispersion as well.

In the harmonic approximation (dots in (2.15) omitted), to be adopted throughout, Eq. (2.15) is that of a hyperparaboloid in the lattice-configurational space \tilde{q} whose minimum is at \tilde{q}_t^0 . For two static electronic states $|i; \tilde{0}\rangle$ and $|j; \tilde{0}\rangle$, the respective paraboloids, at \tilde{q}_i^0 and \tilde{q}_j^0 , intersect along some line L in a hyperplane S . There is a minimum of potential energy at \tilde{q}_{ij} along this line. Insofar as $V_{tt}(\tilde{q})$ represent approximate potential energy surfaces for the vibronic problem, Eq. (2.12) should give the approximate eigenvalues E_{tn} .

Considering energy-conserving "horizontal" transitions from well i to well j , it is intuitively clear that they should proceed along an appropriate line L_p connecting \tilde{q}_i^0 , \tilde{q}_{ij} , and \tilde{q}_j^0 which is the path of minimal potential energy. We shall assume for simplicity that "transition path" L_p to be a straight hyperline, the one along the coordinate q_p of a certain mode. This p -mode will actually promote the transition from i to j and will be called "promoting". The single promoting-mode assumption is not an essential limitation and can be generalized when the motion

along L_p is analyzed in terms of more than one promoting mode, that is, when L_p is a curved line.

The degeneracy in electron energy along the crossover line L violates the adiabatic approximation. One can expect, therefore, the difference between $V_{tt}(\tilde{q})$ and $E_t(\tilde{q})$, the precise eigenvalue of Eq. (2.11), to be most significant around L . That degeneracy is really removed when the electron-transfer interaction between i and j is taken into account.

2.4. Two-state hamiltonian

In order to lift the degeneracy along L , we construct a two-state Hamiltonian H_{ij} by means of the static electronic states $|i; \tilde{0}\rangle$ and $|j; \tilde{0}\rangle$, assumed to be orthonormal:

$$H_{ij} = H_{AD} + K_{ij}(\tilde{q})(|i; \tilde{0}\rangle\langle j; \tilde{0}| + |j; \tilde{0}\rangle\langle i; \tilde{0}|) \quad , \quad (2.21)$$

where $K_{ij}(\tilde{q})$ is a mixing parameter,

$$H_{AD} = H_e + H_{eL} + \sum_1 \frac{1}{2} M_1 \omega_1'^2 q_1'^2 \quad , \quad (2.22)$$

and will seek the eigenvalues of H_{ij} in terms of the linear combination

$$|t; \tilde{q}\rangle = A|i; \tilde{0}\rangle + B|j; \tilde{0}\rangle \quad . \quad (2.23)$$

Solving for

$$H_{ij}|t; \tilde{q}\rangle = E(\tilde{q})|t; \tilde{q}\rangle \quad , \quad (2.24)$$

the eigenvalues are

$$E_{U/L}(\tilde{q}) = \frac{1}{2}(V_{ii}(\tilde{q}) + V_{jj}(\tilde{q})) \pm ((V_{ii}(\tilde{q}) - V_{jj}(\tilde{q}))^2 + 4|(V_{ij}(\tilde{q}) + K_{ij}(\tilde{q}))|^2)^{\frac{1}{2}} \quad . \quad (2.25)$$

Here

$$V_{st}(\tilde{q}) = \langle s; \tilde{0} | H_{AD} | t; \tilde{0} \rangle \quad (2.26)$$

$$= \left(E_t^0 + \sum_1 \frac{1}{2} M_1 \omega_1'^2 q_1'^2 \right) \delta_{st} + \sum_1 (b_{st1} q_1' + c_{st11} q_1'^2 + \dots)$$

are the matrix elements of H_{AD} between states $|s; \tilde{0}\rangle$ and $|t; \tilde{0}\rangle$. In the harmonic approximation $V_{tt}(\tilde{q})$ obtain from (2.15) as well. The matrix elements of the electron-lattice coupling operators are

$$b_{st1} = \langle s; \tilde{0} | \sum_{e,1} b_{e,11}(\vec{r}_e; \tilde{0}) | t; \tilde{0} \rangle \quad (2.27)$$

and

$$c_{st11} = \langle s; \tilde{0} | \sum_{e,1} c_{e,11}(\vec{r}_e; \tilde{0}) | t; \tilde{0} \rangle, \quad \text{etc.} \quad (2.28)$$

Retaining the higher-order terms in the expansion of $\langle s | H_{eL} | t \rangle$ in q_1' is made for the sake of completeness here: usually a linear coupling scheme is adopted neglecting all c_{st11} , etc. The eigen-states of Eq. (2.24) corresponding to $E_{U/L}(\tilde{q})$ have been found to be

$$|t; \tilde{q}\rangle_U = \cos(\psi/2) |i; \tilde{0}\rangle + \sin(\psi/2) |j; \tilde{0}\rangle, \quad (2.29)$$

$$|t; \tilde{q}\rangle_L = -\sin(\psi/2) |i; \tilde{0}\rangle + \cos(\psi/2) |j; \tilde{0}\rangle,$$

with

$$\tan(\psi(\tilde{q})) = 2(V_{ij}(\tilde{q}) + K_{ij}(\tilde{q})) / (V_{ii}(\tilde{q}) - V_{jj}(\tilde{q})) \quad (2.30)$$

Eq. (2.25) defines two adiabatic hypersurfaces, upper $E_U(\tilde{q})$, and lower $E_L(\tilde{q})$. They split by $E_U(\tilde{q}_L) - E_L(\tilde{q}_L) = 2|V_{ij}(\tilde{q}_L) + K_{ij}(\tilde{q}_L)|$ along the crossover line L. Very little is known about the dependence of K_{ij} on the configurational coordinates. Although often assumed constant, a more rigorous treatment would show K_{ij} to be significant along L only and to eventually drop rapidly away from it. Unless the crossover splitting is too large, $E_U(\tilde{q})$ and $E_L(\tilde{q})$ would practically coincide with the corresponding diabatic branches sufficiently far from L. Under the condition of small $|V_{ij}(\tilde{q}) + K_{ij}(\tilde{q})|$ away from crossover, there will be, therefore, two

minima at \tilde{q}_i^0 and \tilde{q}_j^0 on the lower surface, $E_L(\tilde{q})$. However, independent of the magnitude of the splitting there is a valley bottomed along \tilde{L} on $E_U(\tilde{q})$ with its lowest point at \tilde{q}_{ij} , and a corresponding sierra on $E_L(\tilde{q})$ with a bottom bottom at \tilde{q}_{ij} as well. It is now clear why the most favorable transition path connecting \tilde{q}_i^0 and \tilde{q}_j^0 would inevitably pass through \tilde{q}_{ij} .

Cross-sectioned in a plane containing q_p , the potential-energy profile along the promoting-mode coordinate exhibits a barrier peaked at $(q_p)_{ij}$ whose height is

$$E_b = V_{ii}(\tilde{q}_{ij}) - V_{ii}(\tilde{q}_i^0) - |V_{ij}(\tilde{q}_{ij}) + K_{ij}(\tilde{q}_{ij})|$$

$$= \sum_1 \frac{1}{2} M_1 \omega_{i1}''^2 (q_{ij1}'' - q_{i1}''^0)^2 - |V_{ij}(\tilde{q}_{ij}) + K_{ij}(\tilde{q}_{ij})|, \quad (2.31)$$

relative to the minimum of $V_{ii}(\tilde{q})$ at \tilde{q}_i^0 . The difference between the energy minima on $E_L(\tilde{q})$ amounting to

$$Q = Q_j - Q_i = E_j^0 - E_i^0 - \sum_1 \frac{1}{2} M_1 (\omega_{j1}''^2 (q_{j1}''^0)^2 - \omega_{i1}''^2 (q_{i1}''^0)^2), \quad (2.32)$$

according to (2.15) and (2.20), is the "reaction heat" at 0°K. Another important quantity is the "lattice reorganization energy" E_r defined by

$$E_r = V_{jj}(\tilde{q}_i^0) - V_{jj}(\tilde{q}_j^0) = \sum_1 \frac{1}{2} M_1 \omega_{j1}''^2 (q_{i1}^0 - q_{j1}^0)^2. \quad (2.33)$$

This is the average energy gained by the lattice, as two separate wells are created at \tilde{q}_i^0 and \tilde{q}_j^0 through corresponding displacements by virtue of the electron-phonon interaction of a well centered at the origin. Further, from $V_{ii}(\tilde{q}_{ij}) = V_{jj}(\tilde{q}_{ij})$ we get the equation for determining the crossover configuration q_{ij} :

$$\sum_1 \frac{1}{2} M_1 (\omega_{i1}''^2 (q_{ij1}'' - q_{i1}''^0)^2 - \omega_{j1}''^2 (q_{ij1}'' - q_{j1}''^0)^2) = Q. \quad (2.34)$$

The crossover energy at \tilde{q}_{ij} relative to the minimum of $V_{ii}(\tilde{q})$ is

$$E_c = V_{ii}(\tilde{q}_{ij}) - V_{ii}(\tilde{q}_i^0) = \sum_1 \frac{1}{2} M_1 \omega_{i1}''^2 (q_{ij1}'' - q_{i1}''^0)^2. \quad (2.35)$$

It should be stressed that the crossover splitting $E_{U/L}(\tilde{q}_L) - E_L(\tilde{q}_L)$ is composed of dynamic V_{ij} and static K_{ij} parts. Some authors have preferred considering one of these only, while neglecting completely the contribution of the other.^(5,6)

2.5. Vibronic eigenstates

Substituting $E_{U/L}(\tilde{q})$ from (2.25) for $E_t(\tilde{q})$ in Eq. (2.12) and solving it, we obtain the eigenvalues E_{nt} . These represent the total energy of the system in the adiabatic approximation. $E_{U/L}(\tilde{q})$ is the potential-energy surface governing the motion of the lattice oscillators. Insofar as $E_{U/L}(\tilde{q})$ differs from the diabatic hyper-paraboloids in the vicinity of the crossover line L only, E_{nt} and $\chi_{nt}(\tilde{q})$ can be approximated by the energies and eigenstates of harmonic oscillators, respectively ($\xi_{t1} = (M_1 \omega_{t1} / \hbar)^{1/2} q_1$):

$$E_{nt} = \sum_1 \hbar \omega_{t1} (n_1 + \frac{1}{2}) + Q_t \quad , \quad (2.36)$$

$$\chi_{nt}(\tilde{q}) = \prod_1 (\pi^{1/2} 2^{n_1} n_1!)^{-1/2} H_{n_1}(\xi_{t1} - \xi_{t1}^0) \exp - (\frac{1}{2}(\xi_{t1} - \xi_{t1}^0)^2) . \quad (2.37)$$

In fact, (2.36-7) describe vibrational-like states which contain a nearly complete information on the whole system. Actually, E_{nt} comprise not only purely vibrational terms but electronic and lattice-displacement energies as well. On the other hand, the eigenstates $\chi_{nt}(\tilde{q})$ contain information on the displacement, that is, on the magnitude of the electron-phonon interaction. These electron-coupled vibrational states are called "vibronic"; the corresponding entity will hereafter be named "vibron" for short.

A vibron can perform vertical transitions within a well leading to local lattice relaxation through giving away excess energy to the lattice heat reservoir. This relaxation is made possible thanks to the intravibronic coupling terms, accounted for in (2.36) and (2.37) by way of the corresponding frequency dispersion in ω_{t1} (the "superscripts omitted"). What is more important for our purpose, the vibron can also perform horizontal energy-conserving transitions from one well to the other. Such

transitions, leading to the net population of the latter well at the expense of the former, are described in terms of (2.8), which are in fact quasistationary states, being just approximate solutions to Schrödinger's equation (2.7).

2.6. Configurational-coordinate diagrams

A configurational-coordinate diagram is the one which depicts the potential energy of a vibron in one or more electronic states versus the coordinate q of the promoting mode (subscript p hereafter dropped). This is the profile of the vibronic potential energy hypersurface $E_{U/L}(q)$ along the transition path L_p , assumed rectilinear. For the first time now the single-promoting-mode proposition, mentioned earlier, is being put into effect. An example is shown in Fig. 1 with the quantities introduced in Section 2.4 denoted therein. Mathematically, the potential-energy profile in a CC-diagram obtains from (2.25) and (2.26) setting all $q'_1 = 0$ for $1 \neq p$. Depending on the relative strength of the electron-lattice coupling (to which the displacement of the minima are proportional), there are three different types of diagrams distinguished by the relationship between the lattice reorganization energy E_r and the reaction heat Q . From (2.33) and (2.34) we obtain

$$E_r - Q = M_p \omega_p^2 (q_{jp}^0 - q_{ip}^0) (q_{jp}^0 - q_{ijp}^0), \quad (2.38)$$

(subscript p revoked to avoid confusion), account being taken of the fact that under the rectilinearity assumption q_i^0 , q_j^0 , and q_{ij}^0 all lie on the transition line L , which now is one of the coordinate axes, the q_p -axis. For $q_{jp}^0 - q_{ip}^0 > 0$, the three cases are:

- i) Weak coupling ($E_r < Q$, $q_{jp}^0 < q_{ijp}^0$);
- ii) intermediate coupling ($E_r \approx Q$, $q_{jp}^0 \approx q_{ijp}^0$);
- iii) strong coupling ($E_r > Q$, $q_{jp}^0 > q_{ijp}^0$).

Also, from (2.33), (2.34), and (2.35) we obtain the relation

$$E_c = (E_r + Q)^2 / 4E_r \quad (2.39)$$

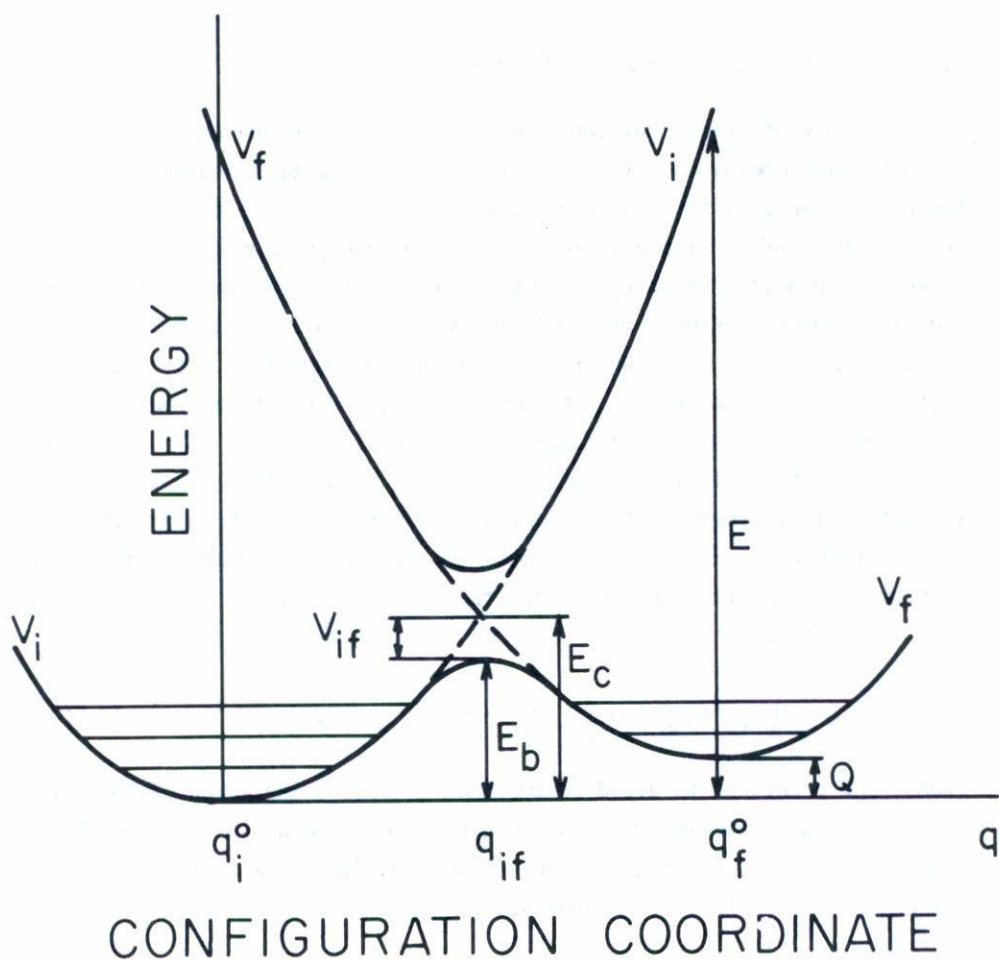


Fig. 1. Potential-energy profile along the promoting-mode coordinate in a strong-coupling situation. The adiabatic energy surfaces are represented by solid lines. The diabatic surfaces are depicted by dashed lines in the vicinity of the crossover (transition) coordinate. Far from crossover these coincide with the corresponding adiabatic branches. See the text for an explanation of the notations. The reaction from left to right is endothermic.

between the crossover and reorganization energies. $E_c = E_r$ for intermediate coupling. The above types of CC-diagram will appear in the experimental examples to be considered below.

3. TRANSITION RATE

3.1. General definition of reaction-rate

The reaction-rate theory provides a method for calculating the rate of horizontal energy-conserving transitions in the two-state model of Section 2. The method is based on an occurrence-probability approach used in Eyring's chemical-rate theory but extended so as to allow for a quantum-mechanical description of the vibrational motion.⁽⁴⁾ The reaction-rate is given by

$$k_{if} = \kappa(T) (k_B T/h) (Z_i^\# / Z_i) \exp(-E_b / k_B T) \quad , \quad (3.1)$$

where

$$\kappa(T) = \sum_n W(\bar{E}_n) \exp(-\bar{E}_n / k_B T) \Delta(\bar{E}_n / k_B T) \quad (3.2)$$

is a quantum correction to the rate equation presented otherwise in a conventional classical form. Here $\bar{E}_n = E_n - E_b$, E_n is the energy of motion along the reaction (promoting mode) coordinate q , \bar{E}_n is the excess of energy relative to the barrier height E_b along q . $W(\bar{E}_n)$ is the total transition probability

$$W(\bar{E}_n) = \sum_{n', n''} W_{n', n''}(\bar{E}_n) F(E_{n'}, T)$$

weighed thermally over the initial state n' , assumed to be in thermal equilibrium, $F(E_{n'}, T)$ being the occupation probability at level $E_{n'}$. More specifically, n' and n'' quantize the motions along the coordinates q_1 of the modes orthogonal to q in the initial (n') and final (n'') states, respectively. As stated in Section 2, the latter modes accept and distribute the excess energy following a horizontal transition through the intra lattice coupling. These shall be called "accepting modes" hereafter. Z_i

is the complete partition function of the initial state,

$$Z_i^\# = \sum_{n'} \exp(-E_{n'}/k_B T) \quad (3.3)$$

is the partition function of the accepting modes in that state. Finally, $\Delta \bar{E}_n = E_{n+1} - E_n$ is the spacing between the subsequent energy levels along the reaction coordinate. k_B , h , and T have their usual meaning. Calculating $W(\bar{E}_n)$ simplifies when q is a normal coordinate of the system; it is then dynamically separable from the domain of all the mode coordinates. In that case $W_{n',n''}$ is independent of the initial-state quantum numbers n' , and summing up over n' would give $W_{n',n''}(E_n)$ so that no thermal averaging is required any more. Now

$$k_{if} = Z_i^{-1} \sum_{n',n''} W_{n',n''}(E_n) \exp(-E_{n'}/k_B T) \exp(-E_n/k_B T) (\Delta E_n/h) \quad (3.4)$$

Equation (3.4) for k_{if} has a simple physical meaning:⁽⁷⁾ While $W_{n',n''}(E_n)$ is the transition probability at energy E_n along the reaction coordinate, $(hZ_i)^{-1} \exp(-E_n/k_B T) \Delta E_n$ can be interpreted as the probability per unit time for an approach to the barrier between the initial and final states along that same coordinate, with energy within the interval ΔE_n . As a matter of fact, the normalized probability that a system would occupy a volume $dq dp_q$ in phase space is $(Z_i h)^{-1} \exp(-E/k_B T) dq dp_q$. In time dt all the phase points within a distance $dq = v_q dt$ from the barrier will strike it; now the desired expression follows since $dp_q = v_q^{-1} dE$. Although using classical arguments for interpreting a quantal formula, the above considerations merely underline the basic result that a "quantum-mechanical rate is given as a sum of probability products in the manner of classical probabilistics."⁽⁷⁾

For a purely classical description one may set simply

$$W(E_n) = \begin{cases} 1, & n \geq n_b \\ 0, & n < n_b \end{cases}, \quad \text{where } n_b = E_b/h\nu - \frac{1}{2} \quad (3.5)$$

From (3.2) converting the sum into an integral one finds $\chi = 1$, and

(3.1) assumes its classical form. For a quantum-mechanical calculation of the relaxation rate, however, knowledge of the transition probability $W(E_n)$ is required. The latter can be found given the potential-energy surface governing the process.

3.2. Transition probability

Generally, the transition probability $W(E_n)$ is defined in terms of the flux of vibrons in the initial electronic state i along the reaction coordinate q towards the transition configuration at q_{if} . This flux is partially reflected back from the barrier and partially transmitted to the final electronic state f . The reverse current back from the final state is neglected, for it is assumed that once in that state the vibron relaxes rapidly to lower levels, giving away the excess energy through its coupling to the accepting modes, so that the chances of return are rather small. Under these conditions,

$$W(E_n) = j_{\text{transmitted}}/j_{\text{incident}} \quad , \quad (3.6)$$

with

$$j(q) = \frac{i}{2} (h\nu/M)^{\frac{1}{2}} \left[\chi \frac{d\chi^*}{dq} - \chi^* \frac{d\chi}{dq} \right]$$

Clearly, $W(E_n)$ can be found by solving the vibronic problem, as formulated by (2.12) and (2.25), in the vicinity of the crossover configuration q_{if} .

To get an idea of the complexity of the problem, we shall seek a solution of Schrödinger's equation (2.7) with $H = T_L + H_{if}$ in terms of the linear combination $\chi_{ni}(q)|i;q\rangle + \chi_{nf}(q)|f;q\rangle = \bar{\chi}_{ni}(q)|i;0\rangle + \bar{\chi}_{nf}(q)|f;0\rangle$ of corresponding adiabatic-approximation wavefunctions pertaining to the initial and final electronic states. Retaining adiabaticity (2.9) and making use of the definitions of Section 2.4 we obtain a system of coupled vibronic equations for $\bar{\chi}_{ni}$ and $\bar{\chi}_{nf}$:

$$\begin{aligned} (E - T_L - V_{ii}(q))\bar{\chi}_{ni} &= (V_{if} + K_{if})\bar{\chi}_{nf} \quad , \\ (E - T_L - V_{ff}(q))\bar{\chi}_{nf} &= (V_{fi} + K_{if})\bar{\chi}_{ni} \quad . \end{aligned} \quad (3.7)$$

These have been solved for $V_{if} = 0$ and $K_{if} = \text{const.}$ assuming linear diabatic potentials in the vicinity of crossover. Clearly, the solutions would tend to the ones pertinent to the diabatic wells, as one moves away from the crossover.

It has been shown that the transition probability can often be represented as a product,

$$W(E_n) = W_L(E_n) W_e(E_n) \quad , \quad (3.8)$$

of the probability W_L for rearrangement of the lattice configuration (displacement of the equilibrium position from q_i^0 to q_f^0) times the probability W_e for a change of the electronic state from i to f . Transitions with $W_e = 1$ are called "adiabatic", while those with $W_e \ll 1$ are "nonadiabatic"; otherwise, intermediate transitions are termed "notadiabatic". Clearly, the electron-transfer factor will depend essentially on the mixing parameter K_{if} or in other words on the magnitude of the adiabatic-energy splitting at crossover: the larger the splitting, the higher W_e and viceversa.

Various expressions have been derived for the transition probability depending on the magnitude of the excess energy $\bar{E}_n = E_n - E_b$ relative to the barrier peak, as well as on whether the energy-surfaces form CC-diagrams of the weakly- or strongly- coupling type. We shall next summarize the formulae obtained so far.

At large positive \bar{E}_n (overbarrier transitions) the lattice rearranges classically, $W_L = 1$. In this case the derived expressions for $W(E_n) = W_e(E_n)$ rest largely on the semiclassical Landau-Zener approach:

$$W_e = 1 - \exp(-2\pi\gamma) \quad , \quad (3.9)$$

where

$$\gamma = (K_{if}^2/2h\nu) (E_n - E_c)^{-1/2} \quad . \quad (3.10)$$

This is the probability for a single passage of the crossing point q_{if} . Equation (3.9) reasonably predicts $W_e \rightarrow 1$ for K_{if} large and $W_e \rightarrow 0$ at vanishing K_{if} .

3.2.1. Strong coupling⁽⁵⁾

Landau-Zener's equation (3.9) has been generalized to account for the possibility of multiple transitions back and forth through the crossover point at $\bar{E}_n \gg 0$:

$$W_e = 2(1 - \exp(-2\pi\gamma))/(2 - \exp(-2\pi\gamma)) \quad (3.11)$$

At $\bar{E}_n \ll 0$ the transition along the reaction coordinate q occurs by nuclear tunneling ($W_L < 1$). A one-way transition probability has been obtained reading (3.8), where

$$W_e = 2\pi\gamma^{2Y} \exp(-2Y)/\gamma\Gamma(\gamma)^2 \quad (3.12)$$

$$W_L = \Pi \frac{F_{n_i n_f}(\xi_0, \xi_c)^2}{2^{n_i + n_f} n_i! n_f!} \exp(-((n_f - n_i)^2 h\nu/E_r) \exp(-E_r/h\nu) \quad (3.13)$$

far below the crossover energy the motion along q being quantized by (2.36). Here n_i and n_f are the vibronic quantum numbers in the initial and final electronic states, respectively, which numbers are chosen so as to satisfy the energy-conservation condition

$$Q = (n_i - n_f)h\nu \quad .$$

Further,

$$F_{n_i n_f}(\xi_f^0, \xi_{if}) = \xi_f^0 H_{n_i}(\xi_{if}) H_{n_f}(\xi_{if} - \xi_f^0) - 2n_i H_{n_i-1}(\xi_{if}) H_{n_f-1}(\xi_{if} - \xi_f^0) + 2n_f H_{n_i}(\xi_{if}) H_{n_f-1}(\xi_{if} - \xi_f^0) \quad (3.14)$$

where

$$\xi = (M\omega^2/h\nu)^{1/2} (q - q_i^0)$$

is the dimensionless phonon coordinate. Eq. (3.13) holds good for $|K_{if}| \ll E_p$. $H_n(\xi)$ are the Hermite polynomials of order n .

3.2.2. Weak coupling⁽¹⁰⁾

At large positive \bar{E}_n (overbarrier transitions) Landau-Zener's formalism yields for the two-way transition probability

$$W_e = 2(1 - \exp(-2\pi\gamma)) \exp(-2\pi\gamma) \quad . \quad (3.15)$$

It vanishes for both large and small K_{if} . The maximum value of W_e is 0.5.

Well under the barrier ($\bar{E}_n \ll 0$) the electron-transfer term is given by

$$W_e = 2\pi\gamma \exp(2\gamma)/\Gamma(1-\gamma)\gamma^{2\gamma} \quad . \quad (3.16)$$

However, its maximum value being 2 at large γ , W_e now does not have the meaning of a probability, as does the product (3.8). For a strongly-quantized system

$$W_L = (F_{n_i n_f}^S / F_{n_i n_i}^W)^2 (2^{n_i} n_i!) / (2^{n_f} n_f!) \exp(2Q/h\nu) \quad , \quad (3.17)$$

which has been derived by a two-fold application of (3.13). Here

$$\begin{aligned} F_{n_i n_i}^W(\xi_{if}) = & 2\xi_{if} H_{n_i}(\xi_{if}) H_{n_i}(-\xi_{if}) - 2n_i H_{n_i-1}(\xi_{if}) H_{n_i-1}(-\xi_{if}) + \\ & + 2n_i H_{n_i}(\xi_{if}) H_{n_i-1}(-\xi_{if}) \quad , \end{aligned} \quad (3.18)$$

while $F_{n_i n_f}^S(\xi_f^0, \xi_{if})$ is given by (3.14).

3.3. *Partition functions*

When the motion along the reaction coordinate q is dynamically separable from the domain of the accepting modes, that coordinate factorizes out from the complete partition function Z_i of the initial state to give

$$Z_i = Z_i^\# \exp(-h\nu/2k_B T) / (1 - \exp(-h\nu/k_B T)) \quad ,$$

where $Z_i^\#$ is the partition function of the nonreactive (accepting) modes.

One obtains

$$Z_i^\# / Z_i = 2 \sinh(h\nu / 2k_B T) \quad (3.19)$$

to be inserted in the general rate equation (3.1). Eq. (3.19) holds good for harmonic vibration along the promoting-mode coordinate.

3.4. Reaction rate

From (3.1) and (3.19) we obtain the rate constant of the present two-site harmonic-vibration model,

$$k_{if} = 2\nu \sinh(h\nu / 2k_B T) \sum_n W_e(E_n) W_L(E_n) \exp(-E_n / k_B T), \quad (3.20)$$

where $\nu = \omega / 2\pi$ is the vibrational frequency of the promoting mode, while n is the vibronic quantum number of the quantized motion along the reaction coordinate. W_e and W_L are the electron-transfer and lattice-rearrangement factors, respectively, $W(E_n) = W_e(E_n) W_L(E_n)$ being the transition probability at energy E_n . For a strongly quantized system ($h\nu \approx E_b$) the relevant formulae for W_L are those given in Section 3.2 which pertain to energies E_n sufficiently far from the barrier top. Near the top or for weakly quantized cases ($h\nu \ll E_b$), quasiclassical techniques have been used in deriving expressions for W_L , described in detail elsewhere.⁽⁵⁾ The semiclassical formulae for W_e obtained so far are reproduced in 3.2. In the strong-coupling case the electron transfer is adiabatic ($W_e = 1$) at large electron-energy splittings K_{if} , and nonadiabatic ($W_e < 1$) otherwise. It is perhaps in this case alone that a probabilistic interpretation applies to W_e . In weak-coupling situations the electron transfer is predicted to always be nonadiabatic ($\max W_e = 0.5$) over the barrier. Another peculiarity in that case is the ultimate value of $W_e = 2$ at large $|K_{if}|$.

The transition from i to f is termed "endothermic" for $Q > 0$, "isothermic" for $Q = 0$, and "exothermic" for $Q < 0$. The transition rates in two opposite directions are simply interrelated:

$$k_{fi} = k_{if} \exp(-Q/k_B T) \quad (3.21)$$

3.5. Correction factor for weakly-quantized systems

We shall herein summarize some results obtained for weakly-quantized systems ($h\nu \ll E_b$) which pertain to nonadiabatic and adiabatic transitions, respectively. The obtained formulae may be found useful in interpreting experimentally observed relaxation rates.

3.5.1. Nonadiabaticity

In case of a strong nonadiabaticity ($|K_{if}| \ll E_b$) resulting from a weak electron-transfer interaction in a transition involving a high barrier the lower-temperature relaxation rates may be too small to be measured. More significant rates occur at higher temperatures, where overbarrier transitions through classical lattice rearrangement ($W_L = 1$) predominate. An Arrhenius temperature behavior results but the observed preexponential factor is much lower than the expected promoting-mode frequency, sometimes by many orders of magnitude.

For a strong-coupling situation the nonadiabatic electron-transfer probability from (3.11) is $W_e = 4\pi\gamma$. Inserting into (3.2) by making use of (3.10), and replacing the sum by an integral we get

$$\kappa(T) = 2(K_{if}^2/h\nu) (\pi^3/E_r k_B T)^{\frac{1}{2}} \quad (3.22)$$

Physically this is an adiabaticity correction to the classical-rate equation equation. Substituting for κ in

$$k_{if} = \kappa(T) (2k_B T/h\nu) \sinh(h\nu/2k_B T) \exp(-E_b/k_B T) \quad (3.24)$$

we obtain a preexponential factor that amounts to

$$2\nu(K_{if}^2/h\nu) (\pi^3/E_r k_B T)^{\frac{1}{2}} (2k_B T/h\nu) \sinh(h\nu/2k_B T)$$

Comparing with the experimentally measured value can serve the purpose of determining $|K_{if}|$.

3.5.2. Classical, intermediate, and quantal vibrons

At the other extreme of sufficiently large $|K_{if}|$ the electron transfer in a strong-coupling situation will be adiabatic ($W_e = 1$). The resulting transition rate can now be expected to be considerably higher at comparable barrier heights than the one considered in 3.5.1. Even though the low-temperature rate may still be too low, the efficiency of the sub-barrier lattice-tunneling transitions at higher vibronic levels will grow increasingly higher as the temperature is raised. Under appropriate conditions the contribution of these tunneling transitions to the overall rate k_{if} may even equal the one of the classical overbarrier jumps at some temperature T_c , wherefrom the classical jumps will grow more and more superior. Clearly, T_c is called "Christov's characteristic temperature" will depend essentially on the shape of the potential-energy profile along the promoting-mode coordinate near the barrier top. Aproximating for that top by an inverted parabola of frequency ν^\ddagger , T_c has been shown to be given by⁽⁸⁾

$$T_c = h\nu^\ddagger / \pi k_B \quad . \quad (3.25)$$

Further, using quasiclassical techniques, the quantum-correction factor to Eq. (3.1) has been found to be⁽⁸⁾

$$\kappa(T) = (\pi/2) (T_c/T) / \sin((\pi/2) (T_c/T)) \quad (3.26)$$

at temperatures $T > \frac{1}{2} T_c$. Numerically $\kappa(T)$ is large near $\frac{1}{2} T_c$ wherefrom it drops down as the temperature is increased to attain values as low as 1 at $T \gg T_c$. Based on these arguments, one can therefore, define the following three temperature ranges of external appearance of an adiabatic vibron:

- i) Quantal ($T < \frac{1}{2} T_c$): lattice tunneling predominating;
- ii) intermediate ($\frac{1}{2} T_c < T < 2 T_c$): lattice tunneling and classical jumps nearly equally effective;
- iii) classical ($2 T_c < T$): classical jumps predominating.

Normally the curvature at the barrier top would exceed that at the well

minima: $v^\# > v$. Consequently, the second and third factors on the right-hand side of Eq. (3.24) would nearly cancel out so that the preexponential factor measured within the intermediate range would exceed the anticipated promoting mode frequency because $\kappa > 1$. Otherwise, the experimental temperature dependence of the rate constant in that range would very closely resemble a straight line in the Arrhenius coordinates. Yet, the magnitude of its intercepts would not only be due to classical but to quantum physics as well.

Although the above profound conclusion of the reaction-rate theory is often underestimated or is simply not taken into account by experimentalists, it substantiates the currently expressed opinion that "the quantum-mechanical tunneling is not an unique property of the low temperatures alone".⁽⁹⁾

In addition to the intercepts, the magnitude of the experimental activation energy E_a in the intermediate range also contains details of the barrier shape due to the quantal effects. Using

$$E_a = - \frac{\partial}{\partial(1/k_B T)} \ln k_{if} , \text{ and}$$

(3.24-6), we obtain assuming $v^\# \gg v$,

$$E_a = E_b - k_B T_c \tag{3.27}$$

around the characteristic temperature. The activation energy determined from Arrhenius plots in the intermediate range is, therefore, lower than the barrier height by an amount proportional to the curvature at the barrier top. This same curvature is also related to the magnitude of the electron-exchange coupling constant $|K_{if}|$:

$$T_c = (h\nu/\pi k_B) (1 + 2E_b/|K_{if}|) , \tag{3.28}$$

as shown recently through differentiating Eq. (2.25) in the vicinity of the crossover configuration.⁽¹¹⁾

The formulae of this Section can be used to analyze experimental

data for the intermediate range aimed at reproducing the potential-energy profile controlling an adiabatic nonradiative transition in a strong-coupling situation. Alternatively, the rate equation (3.24) with quantum-correction factor (3.26) can be regarded as a three-parameter (ν , T_c , E_b) formula, which can be fitted to experimental data by means of an appropriate computer program.

4. APPLICATION

4.1. F center in alkali halides

Among a number of puzzling occurrences at the F center, two old experimental facts have recently inspired renewed theoretical efforts:

- i) The apparent ionizability of the relaxed excited F state (\tilde{F}^*) at low temperature;⁽¹²⁾
- ii) the optical appearance of "ghost" polaron states related to the F center.⁽¹³⁾

The point is that you cannot simply explain (i) in terms of the transition to a conduction-band state, for this would require a positive reaction heat Q making the (endothermic) process physically impossible at low temperature. Then, what if you regard ionization as merely the transition to some appropriate polaron state, assuming that (i) and (ii) are interrelated? Clearly, (i) would follow immediately, provided the latter transition would require negative or no reaction heat at all. This was supported on constructing the configurational-coordinate diagram of the KCl F center by using empirical data on the optical absorption, emission, and ionization energies of F and \tilde{F}^* : Definitely, an exothermic ionization reaction emerged for \tilde{F}^* , involving the possible transition to a virtual polaron state.⁽¹⁴⁾

The \tilde{F}^* ionization rates were next calculated from experimental data on the \tilde{F}^* lifetime and ionization efficiency. When plotted versus the corresponding absolute temperatures, a dependence typical of an exo- or iso-thermic reaction clearly emerged. The pertinent reaction-rate formula was then applied yielding a very satisfactory agreement (Fig. 2.). The

obtained value of the electron-exchange constant $|K_{if}|$, regarded as a fitting parameter, was explained in terms of the transition to a virtual polaron state centered a few lattice spacings away from the vacancy. (14)

A further attempt was then made to pre-calculate a consistent configurational - coordinate diagram of the F center and the bound polaron for a most material where it was expected to work. (15) NaI was chosen, since it was known to couple the F center to a single (A_{1g}) vibrational mode. The semicontinuum model of the F center potential was used, even though somewhat archaic, which was coupled to a A_{1g} -type vibration through modulating both the depth V_o and width r_o of the spherical well by the phonon coordinate q , while leaving the Coulomb tail unchanged,

$$V_e(r,q) = -V_o(r_o,q) (1 - N(r - r_o - q)) - (e^2/\epsilon r) N(r - r_o - q) \quad ,$$

where $N(x)$ stands for Heaviside's step function, and r is the radial electron coordinate. The linear electron-phonon coupling operator was found to be

$$b(r) = \frac{1}{r_o} \left[V_o + \left(\frac{K}{\alpha_M} - 1 \right) V_M + \chi \right] (1 - N(r - r_o)) - \left[V_o - \frac{e^2}{\epsilon r} \right] \delta(r - r_o) \quad ,$$

where $V_o = V_o(r_o,0)$, V_M and α_M are Madelung's potential and constant, respectively, while χ is the electron affinity of the crystal. K is equal to 6 for a breathing-mode type local vibration, and to α_M for the A_{1g} lattice mode. The static electronic problem was solved, and, following the prescriptions of Section 2.3., the diabatic potentials calculated. These are shown in Fig. 3 for the 1s- and 2p- like F bound states, as well as for the 2p- like bound polaron state. The resulting $\dot{C}C$ -diagram is clearly of the type deduced from experimental data for the KCl F center. (14)

4.2. Off-Center impurity dipoles in alkaly halides

The reaction - rate approach was also applied to explaining experimentally measured relaxation rates of off-center dipolar defects, such as Ag^+ , F^- , Cu^+ , and Li^+ , in a number of host materials. From a quantum-mechanical point of view what makes the ion go off-center is the

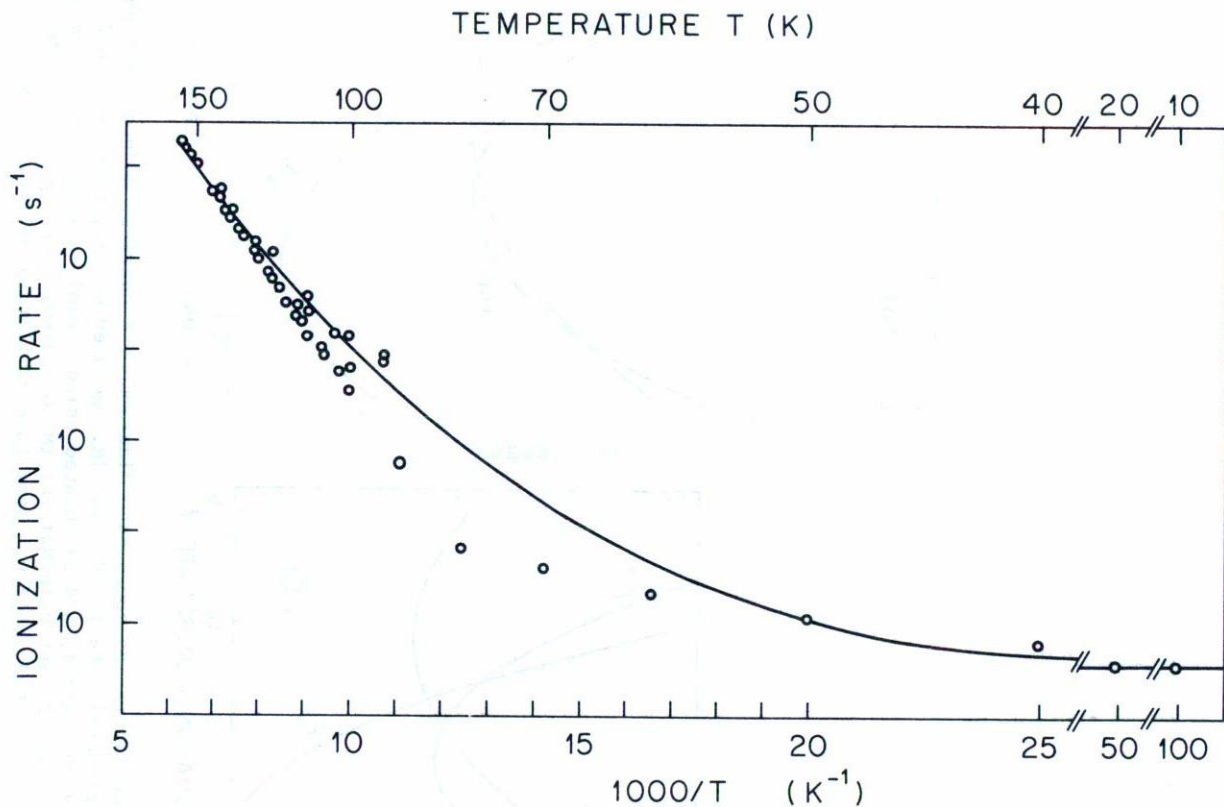


Fig. 2. Ionization rate of the excited F center in KCl. Experimental points from various sources are represented by hollow circles. The solid line is the best fit of Eq. (3.20) for an isothermic reaction. The fitted parameters are: $\omega = \omega_{LO} = 4.02 \times 10^{13} \text{ s}^{-1}$, $E_r = 0.73 \text{ eV}$, $|K_{if}| = 0.01 \text{ eV}$. (After A.D. Gochev, M. Georgiev, and S.G. Christov, *J. Molec. Structure* 115 (1984) 107).

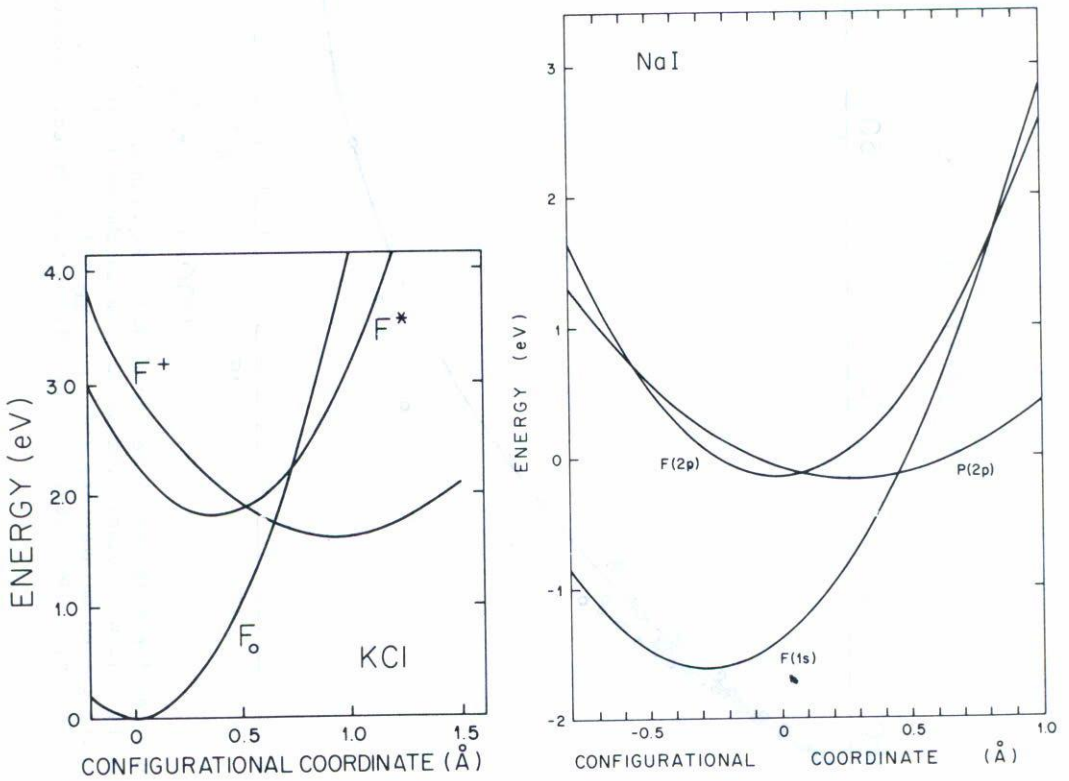


Fig. 3. Configuration-coordinate diagrams of F centers: deduced from experimental data for KCl (a) (M. Georgiev et al., Phys. Rev. B 26, (1982) 6936), and calculated using a semicontinuum vibronic model of the F center in NaI (b) (M. Georgiev, Phys. Rev. B 30 (1984)). Undoubtedly, there is a similarity between (a) and (b).

pseudo - Jahn-Teller interaction.⁽¹⁶⁾ This is properly described by a transition Hamiltonian of the Eq. (2.21) type; however, now the promoting mode, rather than the electron-transfer interaction, mixes the two static states $|i;0\rangle$ and $|f;0\rangle$, already split-of in energy at crossover ($q_{if} = 0$) by $E_{if} = E_f - E_i$:

$$H_{if} = \frac{1}{2} M\omega^2 q^2 - \frac{1}{2} E_{if} (|i;0\rangle\langle 1;0| - |f;0\rangle\langle f;0|) + g_{if} q (|i;0\rangle\langle f;0| + |f;0\rangle\langle i;0|) \quad (4.1)$$

Solving the eigenvalue equation we obtain the following-adiabatic energy in a linear-combination eigenstate (2.23):

$$E_{U/L}(q) = \frac{1}{2} (M\omega^2 q^2 \pm (4 g_{if}^2 q^2 + E_{if}^2)^{\frac{1}{2}}) \quad (4.2)$$

Clearly, these are of the Eq. (2.25) type. A strong-coupling situation results, with lower-surface minima at

$$q_{i/f}^0 = \mp ((4g_{if}^2/2M\omega^2)^2 - E_{if}^2)^{\frac{1}{2}}/2g_{if} \quad (4.3)$$

and a barrier peak at $q_{if} = 0$. The upper surface has a minima at q_{if} . The condition for the occurrence of the minima on $E_L(q)$ is

$$E_{JT} > \frac{1}{4} |E_{if}| \quad (4.4)$$

where

$$E_{JT} = g_{if}^2/2M\omega^2 \quad (4.5)$$

is the Jahn-Teller energy. Under this condition alone is the dipolar off-centered occurrence possible at all. On the other hand, it is the electron-energy splitting at $q_{if} = 0$ what controls the reorientational transition of the dipole from q_i^0 to q_f^0 . Similar conditions apply to Eq. (2.25) if K_{if} is assumed constant. Clearly then, the reaction-rate formulae of Section 3 (strong coupling) are inherently applicable to the off-center

problem, provided $\frac{1}{2}|E_{if}|$ substitutes formally for $|K_{if}|$, and $|b_{ff} - b_{ii}|$ for $|2g_{if}|$.

A best fit of the reaction-rate equation (3.20) to the experimental dipolar relaxation time of off-center Ag^+ in $RbCl$, as measured by nuclear magnetic resonance techniques,⁽¹⁷⁾ is shown in Fig. 4. The off-centered occurrence condition (4.4) is met with abundance.

4.3. Intermediate Eu^{2+} - cation vacancy dipole in KCl

The relaxation time of $\langle 110 \rangle$ symmetry Eu^{2+} - cation vacancy dipoles in a number of alkali halides has been measured by ITC techniques.⁽¹⁸⁾ One of these, the KCl entity, has shown a pre-exponential factor that exceeds by a factor of 2.5 the LO-phonon frequency in the material. In spite of the relatively high temperature of the ITC peak (219°K) and the high activation energy measured (0.66 eV), the data were analyzed in terms of the intermediate dipolar behavior of Section 3.5.2.⁽¹¹⁾ The result is displayed in Fig. 5. The quantal appearance of the entity is predicted to be felt below 150°K but involving relaxation times in excess of 10^{10} s, too long to be measured. The electron-transfer term was computed to be 0.7 eV, using the formulae of Sec. 3.5.2, which clearly indicates an adiabatic behavior. The computed characteristic temperature was 276°K. Believe it or not, quantal effects are sensible in this system at the ice melting point!

4.4. Nonadiabatic hopping of self-trapped exciton in $NaCl$

In an ingenious optical experiment Tanimura and Itoh have determined the hopping rate of a self-trapped excitation in Li^+ doped $NaCl$.⁽¹⁹⁾ The obtained temperature dependence of the rate has been analyzed in terms of Eqs. (3.22) and (3.24), based on an earlier result by Holstein.⁽⁷⁾ A barrier height $E_b = 0.15$ eV and an electron-transfer matrix element $|K_{if}| = 0.022$ eV have been determined. Under these conditions the electron transfer is clearly nonadiabatic, so that the analysis made applies. It is to be stressed that the exciton hopping is basically an isothermic process, as is the dipolar reorientation. Itoh's data and analysis are reproduced in Fig. 6.

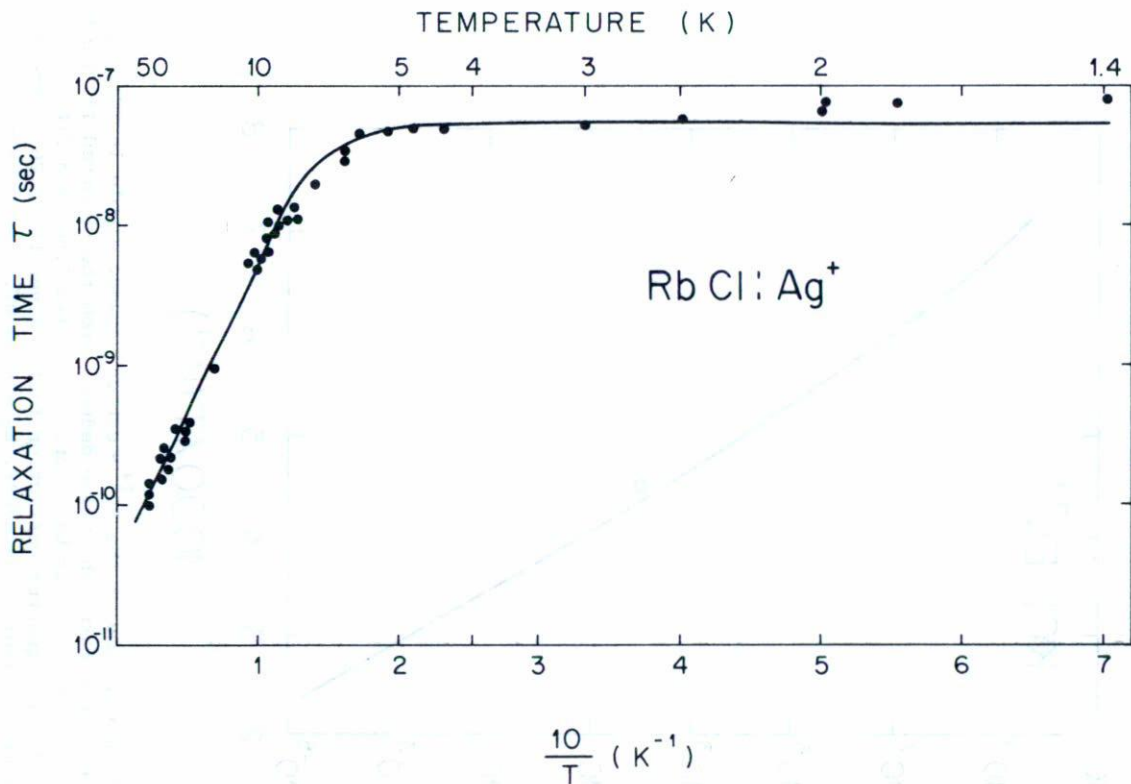


Fig. 4. Relaxation time of the off-center Ag⁺ impurity dipole in RbCl. Experimental points are represented by circles (O. Kanert, Phys. Reports 91, (1982) 183). The solid line is the best fit of Eq. (3.20) for an isothermic reaction. The fitted parameters are: $\nu = 7 \times 10^{11} \text{ s}^{-1}$, $E_T = 0.02 \text{ eV}$, $|K_{if}| = 3.6 \times 10^{-7} \text{ eV}$ (A. Diaz-Gongora et al., to be published).

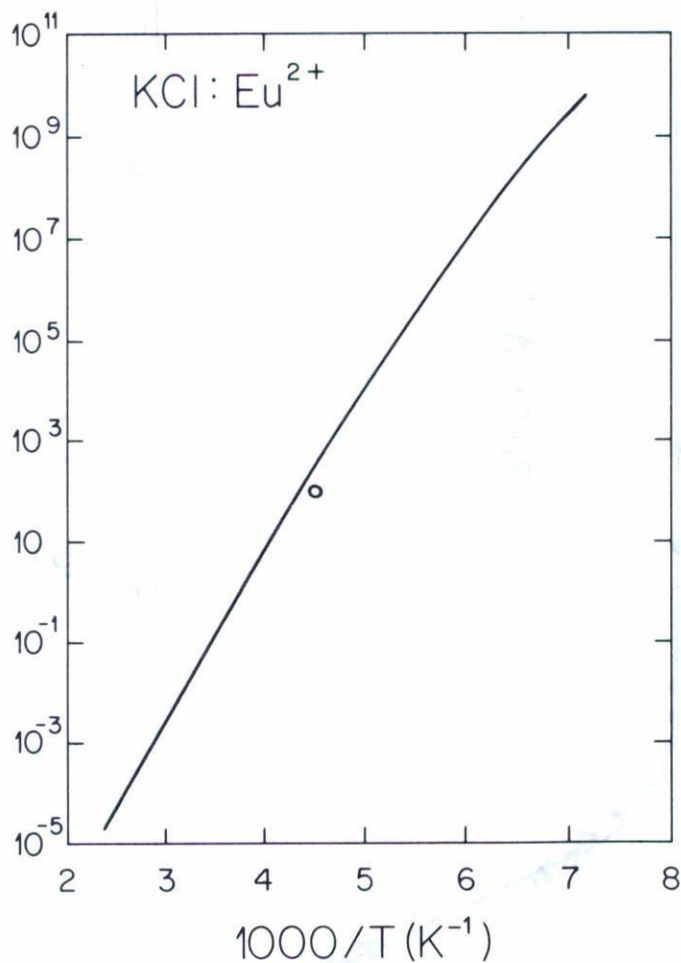


Fig. 5. Relaxation time of the Eu²⁺-cation vacancy dipole in KCl. The sole circle marks the value deduced from the observed ITC band assuming a classical behavior. The solid line is a fit of Eq. (3.24) with quantum-correction factor given by (3.26). The fitted parameters are: $T_c = 276^\circ\text{K}$, $E_b = 0.68 \text{ eV}$, $\nu = \nu_{LO} = 6.39 \times 10^{12} \text{ s}^{-1}$ for an adiabatic reaction. The analysis reveals quantal effects at temperatures as high as the ice-melting point. (After C. Medrano et al., Phys. Rev. B (submitted)).

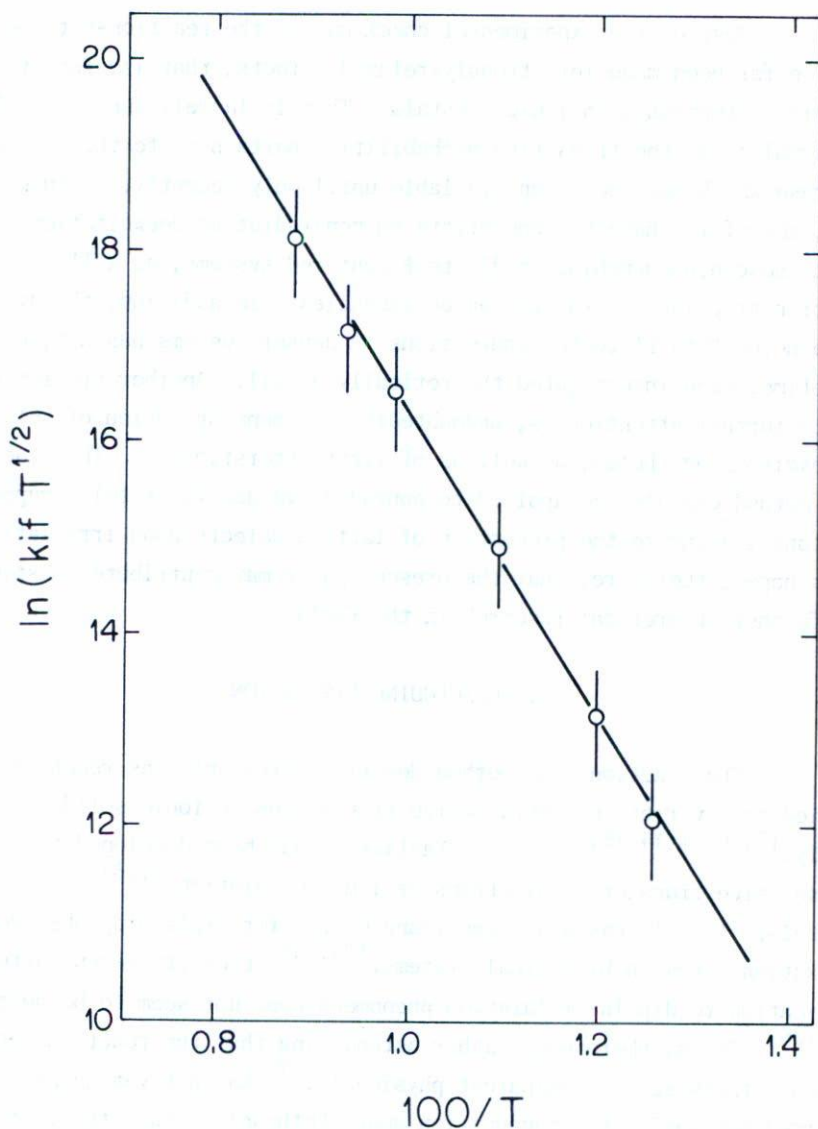


Fig. 6. Hopping rate of self-trapped exciton in NaI. The experimental temperature dependence is analyzed in terms of Eq. (3.24) with a nonadiabaticity correction factor from (3.22). The fitted parameters are $E_b = 0.15$ eV, $|K_{if}| = 0.022$ eV. (After K. Tanimura and N. Itoh, *J. Phys. Chem. Solids* 42 (1981) 901).

4.5. Future perspective

Most of the experimental check-ups of the reaction-rate method have so far been made for strongly-relaxed defects, that is, for strong-coupling situations, in ionic crystals. This is largely due to the lack of formulae for the transition probabilities pertaining to the weak-coupling case which have not been available until only recently. Future work will, therefore, have to concentrate on non-radiative deexcitation leading to luminescence quenching in dilute F centered systems, as well as to electron trapping by isolated anion vacancies. In addition, the dynamics of tunneled F to F' center conversions in denser systems has not, up to this time, been investigated theoretically at all. Another problem which merits further attention is, undoubtedly, the hopping motion of self-trapped excitons and holes, as well as of light interstitials. The reaction-rate method can also be applied to nonradiative decays of self-trapped excitons leading to the production of lattice defects upon irradiation. It is hoped, therefore, that the present paper may contribute to stimulating further theoretical research in the field.

5. CONCLUDING DISCUSSION

The reaction-rate method described presently has recently been applied to a variety of nonradiative transitions in ionic solids mainly. ^(5,10,11,14,15,20,21,22) Earlier it has been developed to deal with nonradiative transfer of electrons or ions in solution ^(4,23) and in molecular crystals. ^(5,7) It has also been found useful for explaining observed relaxation rates in biological systems. ^(24,25) Even its recent attempted application to dipolar relaxation phenomena does not seem to be novel, too. ⁽²⁶⁾ It is, therefore, rather astonishing that the reaction-rate method, otherwise so transparent physically, ⁽⁷⁾ has not yet gained its deserved popularity and recognition among both solid state theorists and experimentalists.

The general formulation of the eigenvalue problem in Section 2, as well as of the transition rate in Section 3, even though taking into account the accepting modes explicitly, was effectively presented under

the single-promoting-mode assumption. At least to some extent, this limitation reflects the present state of the theory, as far as its practical applications are concerned. Clearly, it should by no means be considered a serious obstacle to further extensions and developments, so as to cover more realistic situations, particularly in dipolar relaxation phenomena, when the motion along the reaction path is analyzed in terms of more than one promoting modes. Another limitation was introduced in Section 3, even though not underlined specifically, by assuming that the promoting-mode frequency was essentially the same in both the initial and final electronic states. Although pertaining to certain experimental situations, it does not do so to others, particularly ones of the weak-coupling type. Recently an extension of the Section 3 formulae has been made to two different frequencies in i and f , which is soon to be available in the literature.⁽²⁷⁾

The reaction rate formula (3.20) pertains, let us say it again, to energy-conserving transitions promoted by a single mode, whose frequency does not change along the reaction coordinate, assumed to be one of the normal coordinates of the system. For a strongly-quantized system the relevant expressions for the electron-transfer W_e and lattice-rearrangement W_L factors at energies E_n sufficiently far from the barrier top are those given in Sections 3.2.1 and 3.2.2. For weakly-quantized systems or at energies nearer to the top the appropriate expressions are to be found elsewhere.^(5,10) The resulting equation (3.20) for the transition rate depends on four free parameters: the mode frequency ν , the reaction heat Q , the lattice-reorganization energy $E_x = S h\nu$ (S - the Huang-Rhys factor), and the electron-exchange term $|K_{if}|$ (or the total splitting which includes the dynamic term V_{if} as well, omitted from most of the above considerations). For a symmetric-well potential-energy surface $E_L(q)$ the reaction heat vanishes, so that the number of parameters reduces to three. Symmetric situations of this type pertain to a variety of nonradiative transitions, such as dipolar relaxation, polaron or exciton hopping, diffusion, etc. In comparing the theory with experiment, the rate equation (3.20) has been adapted to the observed rate and the values of the free parameters obtained from the best fit. Clearly, this would not put an end to the theoretical effort which would then have to concentrate on providing independent estimates, based eventually on simple models, to substantiate the best-fit

data. In choosing the type of reaction to explain a particular rate vs. temperature experimental plot, the following consideration may be found useful: exo- or iso-thermic reaction types always lead to nonvanishing low-temperature rates, given by

$$k_{if}(0) = \nu W_e(E_o) W_L(E_o) \dots, \quad (5.1)$$

while endothermic ones end up with vanishing low-temperature rates, according to (3.21), since these would require a positive reaction heat. Whatever the reaction type, however, the occurrence of a non-linear decrease of experimental rate in the Arrhenius plot, as the temperature is lowered, is always indicative of lattice tunneling in situations where the low-temperature rate is too small to be measured.

Finally, by applying relative simple computational techniques to fitting Eq. (3.20), the reaction-rate method may be found to be a useful tool for interpreting experimental rate data.

ACKNOWLEDGEMENTS

The author is greatly indebted to Professor S.G. Christov for introducing and directing him in the field. He is also thankful to Drs. J.L. Boldu and J. Rubio for their hospitality and friendship which both contributed to creating the proper working atmosphere in Mexico City. It was a real pleasure collaborating with such skilful investigators as Drs. A. Gochev, C. Medrano, A. Diaz-Gongora, and J.L. Boldu. The participation of R.J. Gleason in some stages of the work is also appreciated. Useful talks with Drs. B.G. Dick, A.M. Stoneham, R.H. Bartram, D.E. Berry, N. Itoh, F. Bridges, M. Wagner, J. Jortner, and S. Kapphan are also gratefully acknowledged.

REFERENCES

1. A.M. Stoneham, *Theory of Defects in Solids*, Clarendon Press, Oxford, 1975
2. A.M. Stoneham, *Phil. Mag.*, 36 (1977) 983.
3. K. Huang, *Contemp. Phys.*, 22 (1981) 599.

4. S.G. Christov, *Collision Theory and Statistical Theory of Chemical Reactions*, Springer Verlag, Berlin-Heidelberg-New York, 1980.
5. S.G. Christov, *Phys. Rev.*, B 26 (1982) 6918.
6. R. Pässler, *Czech. J. Phys.*, B 32 (1982) 846.
7. T. Holstein, *Phil. Mag.*, B 37 (1978) 49, 499.
8. S.G. Christov, *Ber. Bunsenges. Phys. Chem.*, 79 (1975) 357.
9. A.M. Stoneham, *Internat. Conf. Defects in Insulating Crystals*, Salt Lake City, Utah, 1984 (unpublished).
10. S.G. Christov, *Phil. Mag.*, B 49 (1984) 325.
11. C. Medrano and M. Georgiev, *Phys. Rev.*, B. (submitted).
12. L. Bosi, P. Podini, and G. Spinolo, *Phys. Rev.*, 175 (1968) 1133.
13. F. Borms and G. Jacobs, *Phys. Status Solidi*, 43 (1971) 283; R.C. Brandt, in *Polarons in Ionic Crystals and Polar Semiconductors*, ed. by J.T. Devreese, North Holland, Amsterdam, 1973.
14. M. Georgiev, A. Gochev, A. Kyuldjiev, and S.G. Christov, *Phys. Rev.*, B 26 (1982) 6936.
15. M. Georgiev, *Phys. Rev.*, B 30 (1984)
16. W.B. Fowler, *Radiat. Effects*, 64 (1982) 63; 72 (1983) 27.
17. O. Kanert, *Phys. Reports*, 91 (1982) 183.
18. J.M. Hernández, H. Murrieta S., F. Jaque, and J. Rubio O., *Solid State Commun.*, 39 (1981) 1061.
19. K. Tanimura and N. Itoh, *J. Phys. Chem. Solids*, 42 (1981) 901.
20. A. Gochev, *Solid State Commun.*, 49 (1984) 1181.
21. M. Georgiev and A. Gochev, *Phys. Rev.*, B (accepted).
22. M. Georgiev, *Proc. Internat. Conf. Defects in Insulating Crystals*, Salt Lake City, Utah, 1984 (unpublished).
23. S.G. Christov, *Ber. Bunsen-Gesellschaft*, 76 (1972) 507; 78 (1974) 537; *J. Electrochem. Soc.*, 124 (1977) 69.
24. S.G. Christov, *Internat. J. Quantum Chem.*, 16 (1979) 353.
25. A. Gochev, *Compt. Rend. Acad. Bulg. Sci.*, 31 (1978) 695.
26. R.M. Hill and L.A. Dissado, *J. Phys.*, C 15 (1982) 5171.
27. S.G. Christov, *Phil. Mag.*, B (submitted).